Heteroepitaxial Growth of the Intrinsic Vacancy Semiconductor Al_2Se_3 on Si(111): Initial Structure and Morphology

Chih-Yuan Lu,[1,2] Jonathan A. Adams,[3,*] Qiuming Yu,[2] Taisuke Ohta,[1,2,†] Marjorie A. Olmstead,[3,2] and Fumio S. Ohuchi[1,2,‡]

[1]*Department of Materials Science and Engineering, University of Washington, Seattle, WA 98195-2120*
[2]*University of Washington Center for Nanotechnology, Seattle, WA*
[3]*Department of Physics, University of Washington, Seattle, WA 98195-1560*

(Dated: January 9, 2008)

The evolution of nanostructure morphology and local chemical environment during heteoepitaxial growth of aluminum selenide on Si(111) was investigated with scanning tunneling microscopy and high resolution photoemission spectroscopy. Despite the strong similarity to GaSe in atomic and electronic structure during deposition of the first AlSe bilayer, subsequent growth is quite different, resulting in an alternating Al-Se-Al-Se stacking sequence consistent with defected-wurtzite-structure Al_2Se_3. The first bilayer is completed before additional growth, but subsequent layers nucleate before completion of the second layer. The surfaces of well-formed Al_xSe_y islands are smooth, and terminated by Se atoms, with Al then sticking before additional Se, resulting in rougher, incomplete islands with Al rich, disordered surfaces. Growth with extra Al in the incident flux does not result in layered AlSe, but rather increases the average Al_2Se_3 island size.

PACS numbers: 68.55.ag, 68.35.bg, 68.37.Ef, 79.60.Jv

I. INTRODUCTION

Semiconductors based on compounds consisting of group III and group VI elements are of interest both for the physics associated with their intrinsic vacancy structures and for their significant promise as future device materials. These chalcogenide semiconductors have band gaps and lattice constants similar to those of many more common electronic materials, but their thin film growth is much less studied.[1–11] M_2X_3 compounds (where M=Al, Ga, or In and X=S, Se, or Te) exhibit structures based on the zinc-blende or wurtzite structure of tetrahedrally-bonded III-V and II-VI semiconductors, but in which one-third of the cation sites are vacant. Intrinsic vacancies in the most common structures of bulk Al_2Se_3, Ga_2Se_3 and In_2Se_3 are localized along helices,[12] (also found for γ-In_2Se_3[13,14]), lines[15,16] and planes,[17] respectively. This makes M_2X_3 materials intriguing candidates for functionalization through vacancy ordering (*e.g.*, by creating anisotropic optical properties),[13,18,19] and/or occupation of the vacancies by additional elements (*e.g.* transition metals).[20] The lattice constants of both Ga_2Se_3 and Al_2Se_3 are close to that of Si (0.1 and 1.3% mismatch, respectively), leading to the possibility of combining the unique properties of these intrinsic vacancy materials with silicon technology. Successful application of these materials to silicon technology, however, requires understanding their heteroepitaxy on silicon substrates.

The atomic and electronic structure of the first layer of Al_xSe_y on Si(111)[7] is very similar to that of Ga_xSe_y.[3,4,6,9] Both form a single M-Se bilayer (M = Al, Ga), with Si-M bonding normal to the surface, and an M-Se bond in a direction that continues the diamond (zinc-blende) structure of the substrate (Se in a hollow site). The Si-M and M-Se bond lengths and angles are within 0.02 Å and 2°, respectively, on the two surfaces;[3,4,7] the surface Se exhibits a fully-occupied lone-pair state of similar energy and dispersion on both.[6,7] Despite this similarity in atomic and electronic structure, the AlSe-terminated surface is far more reactive than is GaSe-terminated Si(111). While GaSe/Si(111) does not react under atmospheric exposure, AlSe/Si(111) reacts strongly with O_2, H_2O and atmosphere.[8]

Aluminum and gallium selenides exhibit different bulk structures. Al_2Se_3 and Ga_2Se_3 form defected wurtzite[12] and zincblende[15,16] structures, respectively. Gallium and selenium also exhibit a layered structure, GaSe, with van der Waals bonding between covalently-bonded Se-Ga-Ga-Se layers; InSe takes a similar structure. An equivalent layered structure AlSe, however, has not been reported. The interface bilayers of both AlSe or GaSe on Si have very similar atomic and electronic structure to bulk, layered GaSe,[6] and subsequent growth of Ga_xSe_y on Si(111):GaSe results in layered GaSe.[1] This raises the possibility that layered AlSe may be stabilized through epitaxy on AlSe-terminated Si, Si-Al-Se :: Se-Al-Al-Se, as found for GaSe.

This paper reports a detailed study of the initial stages of Al_xSe_y heteroepitaxy on Si(111) using *in situ* scanning tunneling microscopy (STM) and high resolution core-level photoemission spectroscopy (PES). We find that Al_xSe_y grows in a Al-Se-Al-Se- sequence, consistent with bulk Al_2Se_3 and not a layered AlSe compound, even when an Al_2Se_3 source is supplemented with extra Al. STM reveals the interface AlSe bilayer to be less ordered than GaSe/Si(111),[9] which likely contributes to its increased reactivity. Both STM and PES show a bulk-like Al_2Se_3 structure within the first two layers, including two distinct Se environments and development of bulk-like pho-

toelectron diffraction patterns. Thicker films displayed a $(\sqrt{3} \times \sqrt{3})$R30° low energy electron diffraction pattern.

II. EXPERIMENTAL DETAILS

Experiments were carried out both at the Advanced Light Source (Beamline 7.0.1, Berkeley, CA), for high-resolution core-level PES using synchrotron radiation, and in Seattle, for ultrahigh vacuum STM.[21] X-ray photoemission spectroscopy (XPS) with Mg K_α excitation and low energy electron diffraction (LEED) were performed in both locations to enable direct comparison of film thickness and long-range order on both the bare and covered substrates. Silicon substrates were cut from commercial p-type Si(111) wafers ($\rho \sim 1\ \Omega$−cm) and prepared with repeated chemical etching and oxidation.[7,22] Samples were outgassed in a pressure below a few times 10^{-10} mbar at 725 °C for a minimum of 6 hours. The oxide was then removed by repeated annealing to 1000 °C for 5-10 s, followed by a slow cool to room temperature to obtain a low-defect 7×7 reconstruction. Samples were heated by running a direct current through them; the temperature was monitored using an optical pyrometer.

Aluminum selenide was evaporated from Al_2Se_3 granules heated in a graphite crucible to temperatures between 950 °C and 960 °C, yielding a flux of a few Å/min, as measured by a quartz crystal monitor. The silicon substrate temperature was held constant in the range 550 - 625 °C during deposition. Some experiments also utilized additional Al (Al_2Se_3:Al flux ratio of 1:1) to test whether growth of layered AlSe could be induced by increasing the Al chemical potential.

Photoemission measurements were performed on graded thickness, or wedge-shaped, epitaxial layers of Al_2Se_3 on Si(111) substrates to allow comparison of different thickness films under identical growth and measurement conditions. Wedge samples were grown by moving a shutter across the sample during deposition. The nominal thickness variation over the 50 micron spot size of the synchrotron beam is less than 0.03 bilayers. One bilayer (BL) consists of two Si monolayers or one Al-Se layer, of thickness equal to the minimum (111) step height (bulk Al_2Se_3 BL = 3.17 Å; bulk Si BL = 3.13 Å).

III. RESULTS

Below, we first discuss core-level photoemission results showing the evolution of the stoichiometry and local chemical environments with thickness, followed by detailed STM measurements of both the initial interface bilayer formation and subsequent overlayer growth, with and without extra Al in the incident flux. We also show the development of the band structure with thickness.

A. Core-level Photoemission Spectroscopy

High resolution core level spectra as a function of film thickness are shown in Fig. 1 for both the Si substrate [Fig. 1(a)] and Al_xSe_y overlayer (Al 2p [Fig. 1(b)] and Se 3d [Fig. 1(c)]). The inset schematically shows the wedge sample (0−4 BL). The relative intensities of the fitted components (see below) are shown as a function of position on two wedge samples (0−1 and 0−4 BL) in Fig. 1(d). Due to the strong coverage dependence of the sticking coefficient (much higher for the first layer than the second, then increased again for the third), conversion from position to coverage is only approximate. Lower flux and higher substrate temperatures were used for the thinner sample (see caption).

The unexposed Si shows Si 2p emission characteristic of clean Si(111)7×7 and no Al or Se emission (Fig. 1). As Al and Se begin to stick, the Si 2p attenuates and changes shape until, at about 1 BL thickness, a single, spin-orbit-split component is observed. The narrow Si 2p peak is shifted 0.6 eV to lower binding energy (LBE) relative to the main 7×7 emission, indicating a new Fermi level position close to the valence band maximum. The single component Si, Al and Se spectra at this thickness are equivalent to those previously reported for AlSe-terminated Si(111),[7] and the relative intensity of the Se 3d and Si 2p peaks, measured with Mg K_α XPS, is within our estimated error of that for the well-characterized GaSe bilayer on Si(111).[3,4]

With deposition beyond 1 BL, the Si 2p exhibits no significant change other than attenuation as the overlayer film becomes thicker [Fig. 1(a,d)], while the Al and Se emission each show additional components growing while the interface emission [peaks at position of vertical (blue) lines] is attenuated. A new, broad Al 2p component appears, shifted ∼ 0.9 eV to higher binding energy (HBE) from the original peak. The intensity of this HBE peak [labeled Al I in Fig. 1(d)] steadily increases with thickness, while the original peak (labeled Al 0) attenuates, appearing only as a shoulder at 3−4 BL.

The Se 3d emission [Fig. 1(c)] exhibits two additional components with increasing thickness, but not until the Al I component is well established; the initial Se 0 component is attenuated as the new components grow. One overlayer Se component (labeled Se I) is shifted 0.57 eV to HBE from the original Se 0 component, and the other (Se II) is shifted 0.48 eV to lower binding energy (LBE). The three fitted components are shown for the ∼ 4 BL spectrum in Fig. 1(c) (Se 0 is shaded), with their relative intensities as a function of thickness shown in Fig. 1(d).

Comparison of the intensities of the Si, Al and Se components as a function of position reveals that in the first layer, Al and Se accumulate at roughly the same rate, while in the second layer, Al sticks to the surface before Se. The two bulk Se components (Se I, Se II) begin to appear after the 2nd Al layer nucleates, and increase steadily in a 2:1 ratio with increasing film thickness. The interface Al and Se components (Al 0 and Se 0) are at-

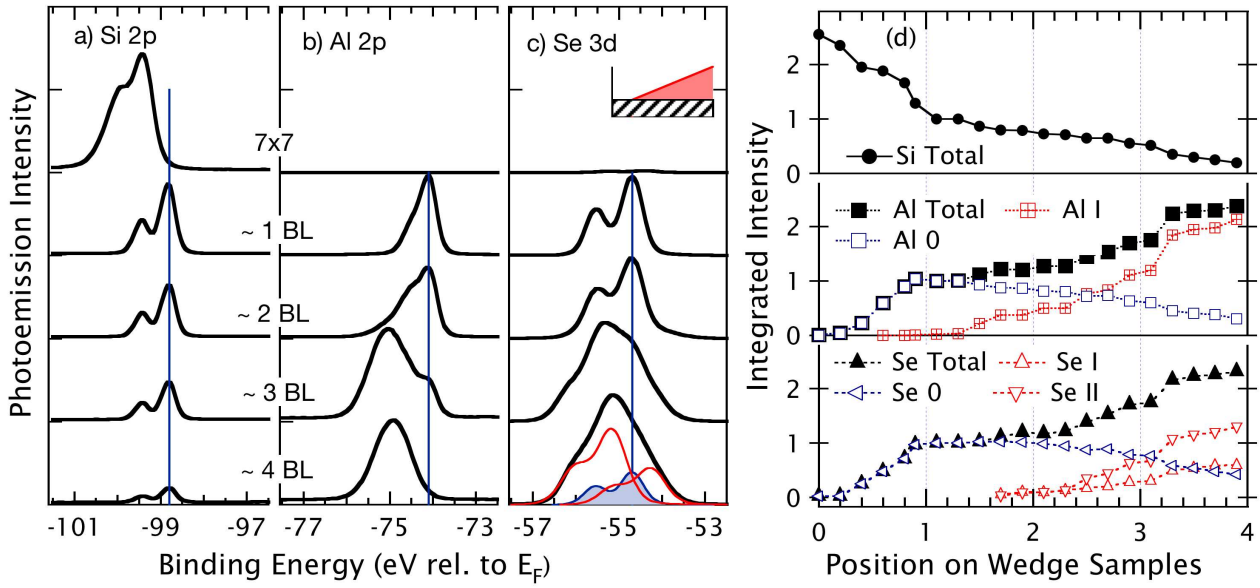

FIG. 1: Photoemission of Al_2Se_3 deposition on Si(111) (color online). (a-c) Spectra from wedge film 0 to 4 BL thick (see inset). Al_2Se_3 flux = 6.5 Å/sec; T_{sub} = 550 °C. Photon energy $h\nu$ = 185 eV. (a) Si 2*p*; (b) Al 2*p*; (c) Se 3*d*. Vertical (blue) lines mark peak ($2p_{3/2}$ or $3d_{5/2}$) for single bilayer. Fitted Se 3*d* components are shown for thickest film. (d) Intensity of fitted components *vs.* position. Component energy was held constant during fitting. Points between 0 and 1 are from a 0-1 bilayer (BL) wedge (Al_2Se_3 flux 1.6 Å/sec, 625 °C, $h\nu$ = 240 eV); points between 1 and 4 are from the same 0−4 BL wedge as (a-c). Position 1 corresponds to a single bilayer for each sample; spectra from both samples are normalized to 1 at this position. Varying sticking coefficients with coverage results in a monotonic, but not necessarily linear, dependence of thickness on position.

tenuated as the overlayer thickness increases.

B. STM of Bilayer Formation

The growth morphology of heteroepitaxial Al_xSe_y on Si was investigated with STM. Given the AlSe stoichiometry found with PES for the first bilayer, despite an Al_2Se_3 source, we supplemented the Al_2Se_3 source with extra Al for the data presented in Fig. 2. The extra Al resulted in better ordering of the surface (see below), but no other significant differences for the first bilayer. Fig. 2 shows STM images from a 39 × 39 nm^2 region of a film deposited with both Al_2Se_3 and Al sources at substrate temperature T_{sub}= 550 °C; the Al coverage is about 1 ML, the Se coverage slightly less. The surface shows two types of regions – "rough" (0.1–0.2 nm corrugation) and "smooth" (∼ 0.01 nm corrugation). The borders of the triangular smooth regions are generally parallel to $\langle 1\bar{1}0\rangle$.

A "smooth" region (upper rectangle) is enlarged in Fig. 2(b), and shows hexagonally symmetric, atomic corrugations similar to those of GaSe-terminated Si(111),[9] where the high points were attributed Se lone pair orbitals. Atomic resolution on this AlSe-terminated surface is much more difficult to obtain and sustain than on GaSe/Si(111). The circle highlights a defect consisting of three bright dots on an equilateral triangle with $\sqrt{3}$ spacing. This defect strongly resembles the most common point defect observed on GaSe/Si(111), labeled D1 in Ref. 9, which is attributed to a point atomic substitution and appears only on domains where the Ga-Se bond is parallel to a Si-Si bond (zinc-blende continuation of the Si lattice). The dark triangle below and to the right of the circled defect resembles a D4-type defect observed[9] on GaSe/Si(111).

An area containing both "rough" and "smooth" regions in Fig. 2(a) (lower rectangle) is enlarged in Fig. 2(c), with a topographic line-scan shown in Fig. 2(d) and a horizontal gradient of the image in Fig. 2(e). The rough region contains arrays of high spots with the same spacing as the adatoms on the starting Si(111)7×7 reconstruction, either ∼0.06 nm or ∼0.03 nm above the neighboring areas, as well as deep holes with the same spacing as the 7×7 reconstructions corner holes [highlighted by rhombus in Fig. 2(c)]. The locations of five bright spots in Fig. 2(c) [along the line scan in Fig. 2(d)] are highlighted with a line of large circles in the gradient image [Fig. 2(e)], while three dimmer spots are highlighted with a triangular array of smaller circles. In these empty state images, the brighter spots are likely Al atoms (with empty p_z orbitals), while the dimmer spots are likely Si adatoms (with singly-occupied dangling bonds). The apparent height difference between the corner holes and the "smooth" region is about 0.32 nm, equal to the bilayer

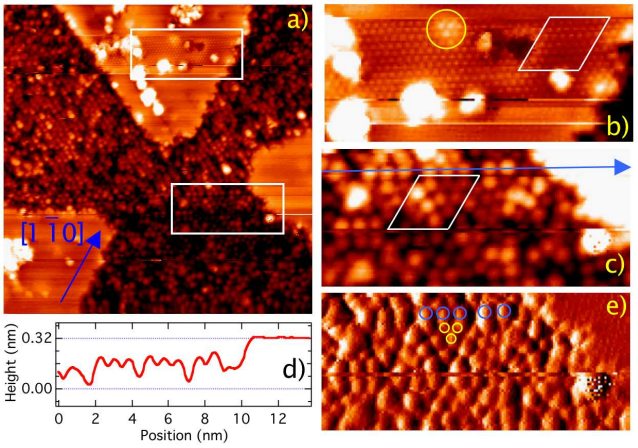

FIG. 2: Bilayer Formation (color online). STM images of ∼ 1 ML Al plus Se, deposited from combined Al_2Se_3 and Al sources at T_{sub} = 550 °C. a) 39 × 39 nm^2 (-2.6 V, 0.12 nA, empty state). b)14 × 6.2 nm^2, enlargement of rectangle in (a), showing atomic resolution of AlSe bilayer; circle highlights a defect similar to the most common defect on GaSe/Si(111); c) 14 × 6.2 nm^2, enlargement of lower rectangle in (a). d) tip height vs. position along line drawn on (c). (e) horizontal gradient of image in (c). Rhombus in (b) and (c) denotes 7×7 substrate unit cell for reference.

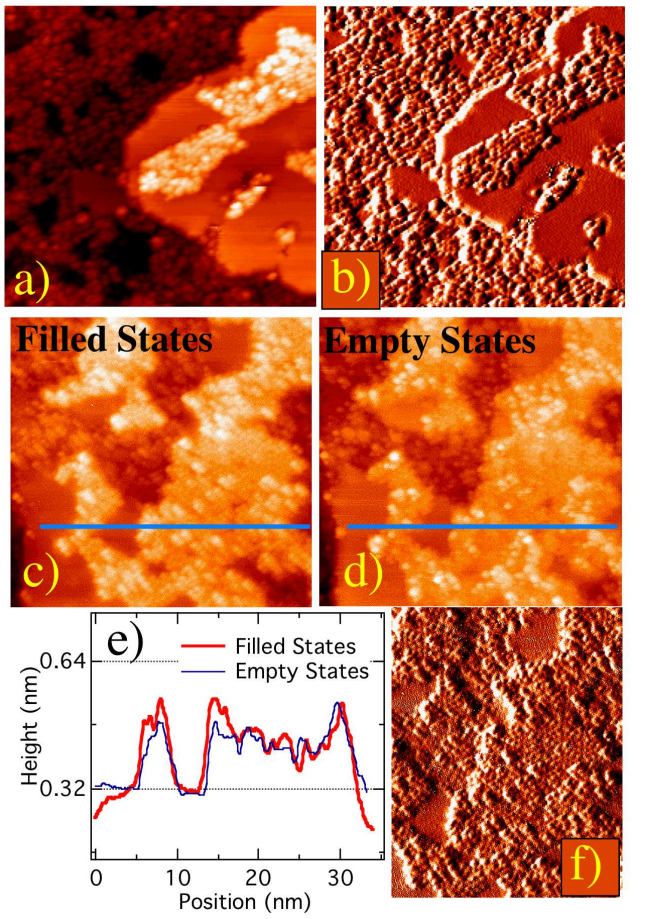

FIG. 3: Overlayer nucleation and growth of Al_2Se_3. (color online) (a) ∼ 1.6 BL Al_xSe_y, deposited at T_{sub} = 585 °C with both Al_2Se_3 and Al sources. 39 × 39 nm^2 (-2.7 V, 0.19 nA). (b) horizontal gradient of (a). (c) ∼ 1.8 BL, dual source, 37 × 37 nm^2 Occupied state image (-2.4 V, 0.16 nA). (d) same region (and color scale) as (c), empty state image (+2.4V, 0.16 nA). (e) height profiles along lines in (c) and (d). (f) horizontal gradient of (d).

step height of Si or Al_2Se_3, while the bright dots (likely adatoms) have an intermediate height, about 0.1 nm below the smooth region. It should be noted that it is unlikely the STM tip measures the true depth of these sub-nanometer diameter "holes."

C. Nucleation of Al_2Se_3 overlayer

The photoemission results (section III.A.) show completion of the first AlSe bilayer before nucleation of additional local environments; similar results are found with STM. Fig. 3 shows STM of about 1.6 BL - 1.8 BL of Al_2Se_3 deposited at T_{sub} = 585 °C. Both Al_2Se_3 and Al sources were used for Fig. 3(a-b); only an Al_2Se_3 source was used for the film in Fig. 3(c-f).

Above 1 BL, the surface again shows "rough" and "smooth" regions, although the "smooth" regions in Fig. 2(a) are now the lower heights on each terrace in Fig. 3(a), while the "rough" regions appear as islands on the smooth background. No evidence of the initial 7×7 structure remains. The lowest areas are similar to the "smooth" regions in Fig. 2, and are presumed to be a complete interface bilayer. The highest points on the "rough" regions are near the height expected for a complete bilayer, with about 0.1 – 0.2 nm corrugation on a 1 – 2 nm length scale. The 2 BL high island at the right of the image in Fig. 3(a) is locally the same as the region surrounding it, evidenced by the gradient image. The island is thus likely a 2 BL high Si island, terminated with an AlSe bilayer and subsequent overlayer nucleation. Small regions 1 BL above the surrounding terrace may also be seen at the edge of the main island.

The effect of the stoichiometry of the incident flux may be seen by comparing Fig. 3(a,b) with Fig. 3(c-f), which are of comparable total thickness (∼ 1.7 BL) with [Fig. 3(a,b)] and without [Fig. 3(c-f)] extra Al. Both show a smooth, completed bilayer as the lowest exposed layer, and both rough and smooth regions. The sample with pure Al_2Se_3 deposition has smaller smooth islands and more dispersed nucleation and growth of the next BL. The local structure of the rough and smooth regions, however, is quite similar under the two deposition conditions [see gradient images Fig. 3(b) and (f)]. The bilayer is covered first by a layer about half the height of a full bilayer. The gradient image in Fig. 3(f) shows a local pattern consistent with a $(\sqrt{3} \times \sqrt{3})$R30° spacing; its height is independent of bias voltage. The highest re-

gions appear to nucleate only when that layer is nearing completion, and look taller in occupied state images than in filled state images.

D. Valence Band

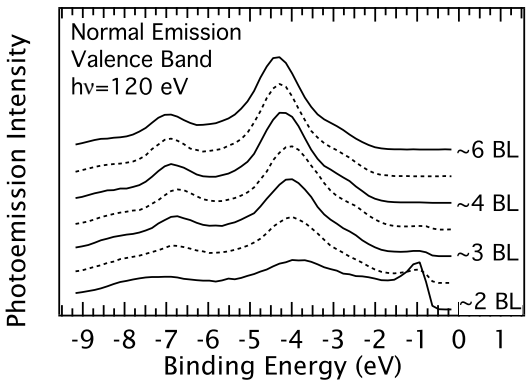

FIG. 4: Development of valence band structure with thickness. Normal emission at photon energy hν = 120 eV. Wedge sample, $\sim$ 2−6 BL, T_{sub} = 550° C, flux = 6.5 Å/min

The development of the valence band structure with film thickness is shown in Fig. 4. The peak just below the Fermi level at low coverage is associated with the Se lone pair emission from the interface AlSe bilayer[7]. In spectra of the pure bilayer at both hν = 130 eV and 21.2 eV, this peak dominates the spectrum.[7,22] This interface peak is no longer visible at a thickness above $\sim$ 3 BL, whereupon bulk-like features, including a shoulder about 2.5 eV binding energy, are established at 2 − 3 BL that are unchanged with further coverage except for a gradual Fermi level shift.

IV. DISCUSSION

The structure of the complete AlSe interface bilayer on Si(111) has been previously shown with photoelectron diffraction[7] to be very similar to that of GaSe/Si(111),[3,4] although it is much more reactive.[8] We have also found that the range of temperature and flux for which the growth self-limits at a single bilayer is much narrower for Al_xSe_y growth than for GaSe deposition.[22] Fig. 2(b) shows the local structure, including even the point defects of the completed AlSe/Si(111) bilayer, to be similar to GaSe/Si(111), but the uniformity and stability are inferior on the AlSe-terminated surface. The large number of defects and rough island edges on the surface likely accounts for the increased reactivity of AlSe/Si(111) over GaSe/Si(111). The increased affinity for adsorbates likely also contributes to the difficulty in obtaining high resolution images of the AlSe bilayer structure.

The PES measurements, where films were deposited with a single Al_2Se_3 source, show Al and Se sticking more-or-less simultaneously for the first BL. In the case of dual source deposition (Al + Al_2Se_3), STM shows that Al first occupies adatom sites in the Si(111)7 × 7 structure, and then joins with Se to form a completed bilayer. Adatoms on the Si(111) surface bond to three Si dangling bonds, so that trivalent Al has a larger contribution to empty-state than to filled-state images, while tetravalent Si is similar in each, leading to our association of the bright spots in the empty-state image of Fig. 2 with Al adatoms at sub-monolayer coverage.

After completion of the first bilayer, the second layer begins to nucleate (Fig. 3). The initial layer appears similar in height in both filled and empty state images, while the regions where the layer is highest are taller in filled state images. This is consistent with the PES results indicating that a significant fraction of an Al layer sticks to the completed bilayer before second-layer Se begins to stick, even with a single source. Al in a $(\sqrt{3} \times \sqrt{3})$R30° structure on AlSe-terminated Si(111), which exhibits no dangling bonds, would be expected to exhibit both full and empty states, while Se bonding to this structure should have more occupied states. The step heights observed in STM are those of a single bilayer (0.32 nm), and not the quad-layer ($\sim$ 0.8 nm) associated with layered III-VI materials. The larger islands and better order observed for growth with extra Al may be attributed to faster diffusion on a surface with excess Al. While Al sticks before Se, it appears to self-limit to a film that is locally 1 ML or less. Once that is completed, the Se can stick and complete the bilayer. This initial sticking of Al, combined with the absence of a layered bulk AlSe phase (from which we infer that AlSe has a higher energy than Al_2Se_3), preclude nucleation of layered AlSe, even though the first bilayer has a lone-pair termination similar to layered GaSe.

Photoemission shows the second layer already displays distinct, bulk-like chemical environments − one bulk environment for Al atoms and two for Se. The bulk valence band structure starts with the second bilayer and is established by the third (Fig. 4). These same environments persist to very thick films. Our XPS measurements on films (Al_2Se_3 source) over 8 nm thick show two Se 3d components separated by 1.06±0.02 eV with a ratio 2.15 : 1 in normal emission and photoelectron diffraction signatures consistent with wurtzite; the energy difference Δ_{Al-Se} between the Al $2p_{3/2}$ and Se I $3d_{5/2}$ is 19.76 ± 0.04;[22] the two bulk-like Se components in Fig. 1(b) are separated by 1.05 ± 0.02 eV, and Δ_{Al-Se}=19.79 ± 0.04 eV for the equivalent bulk-like components. In bulk Al_2Se_3 there are two distinct Se sites: 2/3 of the Se atoms have three Al atoms and one Al vacancy as nearest neighbors, while the remaining 1/3 of the Se atoms are adjacent to two Al atoms and two vacancies. Similar chemical environments have been observed in growth of defect zinc-blende Ga_2Se_3/Si(100), where Ga has one chemical site and Se has two chemical sites arising from the same

nearest neighbor environment as for the wurtzite structure; the separation between the two Se 3*d* components is again just over 1 eV.[10] Angle-resolved valence band spectra taken with $h\nu = 21.2$ eV on an 8 nm Al_2Se_3 film showed weakly dispersing states at ∼2.5 and ∼4 eV below the Fermi level, similar to the $\vec{\mathbf{k}} = 0$ states in Fig. 4. These results show the local structural and electronic environment of Al_2Se_3/Si(111) is established in the first 2-3 bilayers.

In bulk Al_2Se_3, the intrinsic vacancies form a $(\sqrt{3} \times \sqrt{3})$R30° pattern in the (0001) plane (equivalent to the (111) plane of zinc-blende). We observed a $(\sqrt{3} \times \sqrt{3})$R30° LEED pattern on thick (8 nm) films, but observed neither any obvious vacancy-induced reconstruction with STM nor LEED superstructure on thin ($\lesssim 2$ nm) films. It thus appears that the vacancy ordering requires at least a few unit cells to become established.

V. SUMMARY

Despite the strong similarity between the interface bilayer of GaSe/Si(111) and AlSe(111), as previously established with photoemission and confirmed here with atomic resolution STM, growth of subsequent layers is quite different. The combination of scanning tunneling microscopy, core-level photoemission and valence band photoemission data shows that a local Al_xSe_y structure similar to the bulk, defected-wurtzite structure is established, in contrast to the layered GaSe obtained under similar conditions for GaSe/Si(111). After completion of the first bilayer, the film grows by Al sticking first and then Se completing the layer locally. The local environment is similar with either pure Al_2Se_3 or mixed Al_2Se_3 + Al sources, although larger islands are found with extra Al. Even when extra Al is added to the incident flux, a layered AlSe film is not produced. Rather, the overlayer structure continues to take the III-VI stacking sequence (Al-Se-Al-Se). Supplying extra Al leads to larger islands that are more widely spaced (likely due to a longer diffusion length).

Acknowledgments

This work was supported by NSF Grants DMR-0102427 and 0605601 and the M. J. Murdock Charitable Trust. T.O further acknowledges support from the UW-CNT University Initiative Fund. Some data were obtained at the Advanced Light Source in Berkeley, CA (DOE Contract No. DE-AC03-76SF00098). J. A. A. and C.-Y. L. submitted portions of this work in partial fulfillment of the requirements for the Ph.D. at UW.

---

* Present address: Advanced Portfolios Ltd., London
† Present address: Advanced Light Source, Lawrence Berkeley National Laboratory, Berkeley, CA 94720.
‡ Electronic address: ohuchi@u.washington.edu

[1] Le Thanh Vinh, M. Eddrief, John E. Mahan, André Vantomme, J. H. Song, Marc-A. Nicolet, J. Appl. Phys. **81**,7289 (1997).
[2] A. Koebel, Y. Zheng, J. F. Pétroff, J.C. Boulliard, B. Capelle, and M. Eddrief, Phys. Rev. B **56**,12296 (1997).
[3] S. Meng, B. R. Schroeder, and M. A. Olmstead, Phys. Rev. B **61**, 7215 (2000).
[4] S. Meng, B. R. Schroeder, A. Bostwick, E. Rotenberg, F. S. Ohuchi, and M. A. Olmstead, Phys. Rev. B **64**, 235314 (2001).
[5] R. Rudolph, C. Pettenkofer, A. Klein, and W. Jaegermann, Appl. Surf. Sci. **167**, 122 (2000).
[6] R. Rudolph, C. Pettenkofer, A. A. Bostwick, J. A. Adams, F. S. Ohuchi, M. A. Olmstead, B. Jaeckel, A. Klein, and W. Jaegermann, New J. Phys. **7**, 108 (2005).
[7] J. A. Adams, A. Bostwick, T. Ohta, Fumio S. Ohuchi, and Marjorie A. Olmstead, Phys. Rev. B **71**, 195308 (2005).
[8] J. A. Adams, A. Bostwick, Fumio S. Ohuchi, and Marjorie A. Olmstead, Appl. Phys. Lett. **87**, 171906 (2005).
[9] Taisuke Ohta, Andreas Klust, Jonathan A. Adams, Qiuming Yu, Marjorie A. Olmstead, and Fumio S. Ohuchi, Phys. Rev. B **69**, 125322 (2004).
[10] Taisuke Ohta, Diedrich A. Schmidt, Shuang Meng, Andreas Klust, Aaron A. Bostwick, Qiuming Yu, Marjorie A. Olmstead, and Fumio S. Ohuchi, Phys. Rev. Lett. **94**, 116102 (2005).
[11] Fumio S. Ohuchi and Marjorie A. Olmstead, Thin Film Growth of III-VI Semiconductors, Encyclopedia of Electrical and Electronics Engineering, John G. Webster, ed. (John Wiley and Sons, New York, 1999).
[12] A. Schneider, G. Gattow, Z. Anorg. allg. Chem. **277**,49 (1954).
[13] J. Ye, T. Yoshida, Y. Nakamura and O. Nittono, Appl. Phys. Lett. **67**,3066 (1995).
[14] J. Ye, S. Soeda, Y. Nakamura and O. Nittono, Jpn. J. Appl. Phys. **37**,4271 (1998).
[15] D. Lübbers, B. Leute, J. Sol. St. Chem., **43**,339 (1982).
[16] M. Peressi, A. Baldereschi, J. Appl. Phys. **83**,3092 (1998).
[17] M. Ishikawa and T. Nakayama, Jpn. J. Phys. **36**,L1576 (1997).
[18] T. Okamoto, N. Kojima, A. Yamada, M. Konagai, K. Takahasi, Y. Nakamura, and O. Nittono, Jpn. J. Appl. Phys. **31**,L143 (1992).
[19] T. Nakayama and M. Ishikama, J. Phys. Soc. Jpn. **66**,3887 (1997).
[20] C.-S. Yoon, K-.H. Park, D.-T. Kim, T.-Y. Park, M.-S. Jin, S.-K. Oh and W.-T. Kim, J. Phys. Chem. Sol. **62**,1131 (2001).
[21] Omicron Variable Temperature UHV Scanning Probe Microscope.
[22] J. A. Adams, Ph.D. thesis, University of Washington (2004).